第35卷 第4期
2013年12月
地 震 工 程 学 报
CHINA EARTHQUAKE ENGINEERING JOURNAL
Vol.35 No.4
Dec,2013

2013年岷县漳县M_S6.6地震滑坡特征参数分析

田颖颖[1,2]，许 冲[1]，徐锡伟[1]，陈 剑[2]

（1. 中国地震局地质研究所，活动构造与火山重点实验室，北京 100029；
2. 中国地质大学（北京）工程技术学院，北京市海淀区学院路29号，北京 100083）

摘要：2013年7月22日，甘肃岷县、漳县发生了M_S6.6地震。震后遥感影像目视解译与实地调查结果表明，本次地震触发了至少2 330处滑坡，大概分布在一个面积为330 km²的矩形区域内。本文在GIS平台下统计了这些滑坡的发生高程、坡度、坡向、斜坡曲率、地层岩性、PGA共6类地形、地质与地震特征参数的特征。结果表明2 400 m~2 600 m的高程范围、10°~20°的坡度范围、西与北西坡向、-1~-0.1斜坡曲率值范围、古近系（E^b）砾岩与砂岩中、地震动峰值加速度（PGA）为0.16 g是岷县漳县地震滑坡的多发因子区间。

关键词：岷县漳县地震；地震滑坡；特征参数

中图分类号：P315.942；P642.22　　**文献标识码**：A　　**文章编号**：1000-0844(2013)04-761-07

DOI：10.3969/j.issn.1000-0844.2013.04.761

Analysis of Parameters of Landslides Triggered by the Minxian-Zhangxian M_S6.6 Earthquake

TIAN Ying-ying[1,2], XU Chong[1], XU Xi-wei[1], CHEN Jian[2]

(1. Key Laboratory of Active Tectonics and Volcano, Institute of Geology, CEA, Beijing 100029, China;
2. College of Engineering and Technology, China University of Geosciences, Beijing 100083, China)

Abstract: On July 22, 2013 at 07:45 (Beijing time), an earthquake of M_S6.6 occurred at the boundary between Minxian County and Zhangxian County in the mountain area of Western Qinling, southern Gansu Province. A strong aftershock of M_S5.6 occurred at 34.6°N, 104.2°E at a focal depth of 14 km. As of 13:00 24 July, the earthquake had affected 780 100 000 people in 491 towns of 33 counties in 6 cities (prefectures): Dingxi, Longnan, Tianshui, Baiyin, Linxia, and Gannan. The earthquake caused 95 deaths and 1 366 injuries. The earthquake triggered many landslides for several reasons, including that the earthquake-struck area in the western Qinling area of southern Gansu Province was covered by loose thick loess and has steep topography, and there was strong rainfall before the earthquake. Strong aftershocks caused more landslides to occur. The landslides triggered by the Lushan earthquake were of various types, such as falls, slides, and topples on loess scarp, soil deep-seated landslides, large soil avalanches, and slope cracks. From visual interpretation of post-earthquake remote sensing images and selected field checks, at least 2 330 landslides were triggered by this earthquake, and these landslides occurred in a rectangular area of about 330 km². Based on the geographic information system (GIS), we analyzed six topographic, geological, and seismic parame-

收稿日期：2013-08-27
基金项目：国家自然科学基金项目（41202235，91214201）；中国地震局地质研究所基本科研业务专项资助（IGCEA1215，IGCEA1302）
作者简介：田颖颖（1989-），女，硕士研究生，研究方向为滑坡 危险性评价.
通讯作者：许 冲（1982-），男，副研究员，研究方向为地震滑坡与活动构造. E-mail：xc11111111@126.com

ters: elevation, slope angle, slope aspect, slope curvature, formation lithology, and PGA. The elevation of the study area ranges from 2 207 m to 3 340 m. The study area was divided into 11 classes based on 200 m intervals for landslide statistics. The slope angles in the study area range from 0° to 64.6°, and were divided into nine classes: 0°~5°, 5°~10°, 10°~15°, 15°~20°, 20°~25°, 25°~30°, 30°~35°, 35°~40°, and 40°~64.6°. The slope aspect was divided into nine classes: flat, north, northeast, east, southeast, south, southwest, west, and northwest. Based on the slope curvature value, the study area was divided into six classes, and the ranges of the slope curvature value were <−1, −1 to −0.1, −0.1 to 0, 0 to 0.1, 0.1 to 1, and >1. The six categories of strata in the study area are: (1) Q_4, Q_4^{czh}, Q_3; (2) N^b; (3) E^b; (4) P_1^{1-c}; (5) P_1^{1-b}, P_1^{1-a}, (6) D_3^{dc}, and (7) D_2^{2-e}. The PGA values for the study area were divided into eight classes: 0.34 g, 0.32 g, 0.28 g, 0.24 g, 0.2 g, 0.16 g, 0.12 g, and 0.08 g. Analysis of the topographic parameters showed that the Minxian − Zhangxian earthquake-triggered landslides mostly occurred in areas with these characteristics: an elevation between 2 400 m and 2 600 m, a slope angle between 10° and 20°, a W or NW slope aspect, and a slope curvature between −1and−0.1. The Paleogene sandstones and conglomerates (E^b) suffered more landslides. The statistics of the peak ground acceleration (PGA) showed that 0.16 g is the PGA for most of the earthquake-triggered landslides. This paper can show which topographic, geological, and earthquake factors were linked with landslide occurrence. The point-based inventory of landslides triggered by the Minxian − Zhangxian earthquake can provide basic data for subsequent studies of earthquake-triggered landslides, such as spatial distribution analysis, hazard assessment, and mitigation of landslides and debris flows in earthquake-struck areas.

Key words: Minxian−Zhangxian *M*s6.6 Earthquake; earthquake landslide; parameters

0 引言

2013年7月22日7时45分55.1秒，在我国甘肃省定西市岷县、漳县交界处(34.5°N，104.2°E)发生了*M*s6.6地震，震源深度20 km。此次地震共造成定西、陇南、天水、白银、临夏、甘南6个市(州)的33个县(区)、491个乡(镇)、78.01万人受灾。

地震滑坡是危害较大的地震次生灾害，大地震往往导致大量地震滑坡的发生[1]，如1929年新西兰 M_W 7.7默奇森地震[2-3]、1976年危地马拉 M_W 7.5地震[4]、1989年美国加州洛马普列塔 *M*w 6.9地震[5]、1994年美国加州 M_W 6.7北岭地震[6]、1999年中国台湾南投 M_W 7.6集集地震[7]、2008年中国汶川 M_W7.9地震[8-12]、2010年 M_W6.9中国玉树地震[13-15]、2010年海地太子港 M_W7.0地震[16-18]、2012年新疆和静、新源交界 M_S6.6地震[19]、2013年芦山 M_S7.0地震[20-22]等。本次地震震区位于甘肃南部西秦岭山区，山大沟深，道路狭窄，属于滑波、泥石流地质灾害易发地区。据现场初步调查，地震导致了极震区产生了大量的滑坡灾害[23]。

研究地震滑坡特征参数的分布规律可以得到地震滑坡的影响因子多发区间，为地震区滑坡与泥石流防灾减灾提供科学依据。本文在GIS平台下，依据震后遥感影像目视解译方法，并结合部分滑坡实地调查，得到本次地震触发的2 330处滑坡位置；统计了这些滑坡的发生高程、坡度、坡向、斜坡曲率、地层岩性、PGA共6类地形、地质与地震特征参数的分布特征。

1 2013年岷县漳县地震滑坡概况

岷县漳县地震震区位于南北地震带北端的甘东南地区，是中强震多发区，历史上和现今中强地震时有发生，近十年以来在该地区发生了多次5级以上地震，也是近年地震监测关注的地区。此次地震发生在临潭 - 宕昌断裂附近，该断裂由多条规模不等、相互平行或斜列的次级断裂组合而成，断裂带影响宽度范围在5~10 km，在岷县东南部断裂归并为一体，延至宕昌以南。断裂的总体性质是以向北逆冲为主，略具左旋走滑分量。断裂呈NW - NNW向展布，倾向NE，倾角50°~70°，为晚更新世 - 全新世活动断层[24]。研究表明，岷县漳县地震的震源破裂方向是由SEE向NWW方向发展的(中国地震局地球物理研究所，www.cea-igp.ac.cn)。图1为岷县漳县地震区域构造图，区内主要构造方向为NW - SE方向。

由于岷县漳县地震震区位于甘肃南部的西秦岭山区，覆盖较厚的松散黄土层，地形比较陡峻，地震前后又有较强的降雨过程，产生了地震与降雨耦合作用[25]。再加

上此次地震主震和强余震的作用，这次地震诱发了大量的滑坡[23]。这些滑坡主要分为4类：(1)黄土崖崩、滑、倾破坏；(2)深层连贯型土质滑坡；(3)大型土质流滑；(4)斜坡裂缝。本文根据野外调查，基于地震前后高分辨率遥感影像，开展了岷县漳县地震滑坡解译工作，建立了岷县漳县地震滑坡点数据库[26]，库内共包含2 330条用点要素示的地震滑坡记录，主要分布在一个面积约330 km²的矩形区域内。图2为两组地震滑坡照片与影像对比，图2a与2(b)中滑坡对应的照片分别为图2(c)与图2(d)。图3为岷县漳县地震触发的滑坡分布图。

2 滑坡控制变量的统计分析

地震滑坡的发生受多个因素的影响，总体包括地形因素、地质因素与地震因素3个方面。我们选择了高程、

F_1：临潭－宕昌断裂；F_{2-1}：西秦岭北缘断裂漳县段；F_{2-2}：西秦岭北缘断裂锅麻滩段；F_3：洮河断裂；F_4：马衔山北缘断裂；F_5：光盖山－迭山北麓断裂；F_6：光盖山－迭山南麓断裂；F_7：白龙江断裂；F_8：礼县－罗家堡断裂。

图1 岷县漳县地震区域构造图

Fig.1 Regional tectonic setting of the 2013 Minxian－Zhangxian earthquake

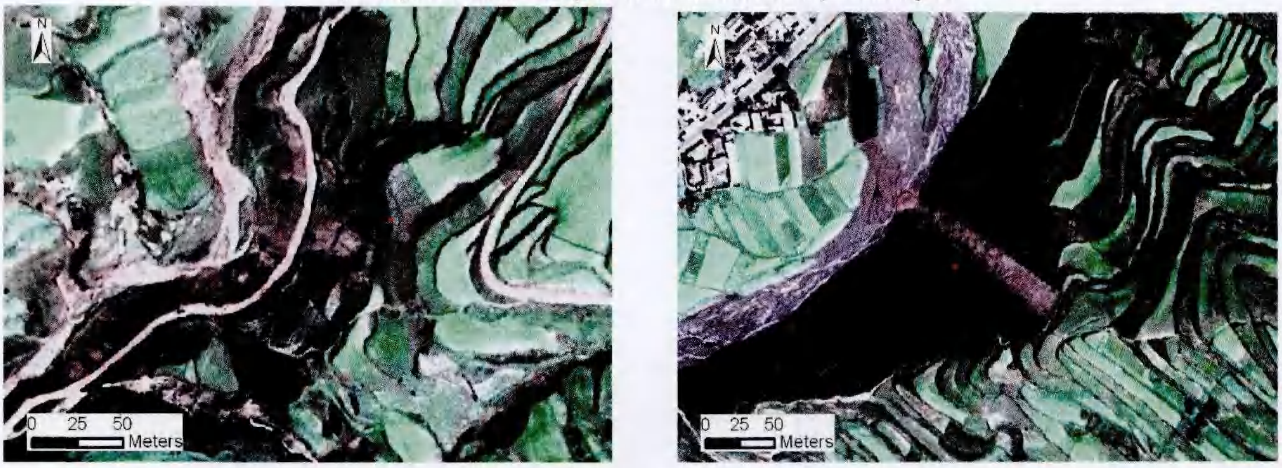

(a) 滑坡A的影像　　(b)滑坡B的影像

(c) 滑坡A的照片　　(d)滑坡B的照片

图2 岷县漳县地震触发的两个滑坡的遥感影像与照片(红点代表滑坡的位置)

Fig. 2 Comparison of satellite images and photos of two landslides. (Red points show locations of the two landslides)

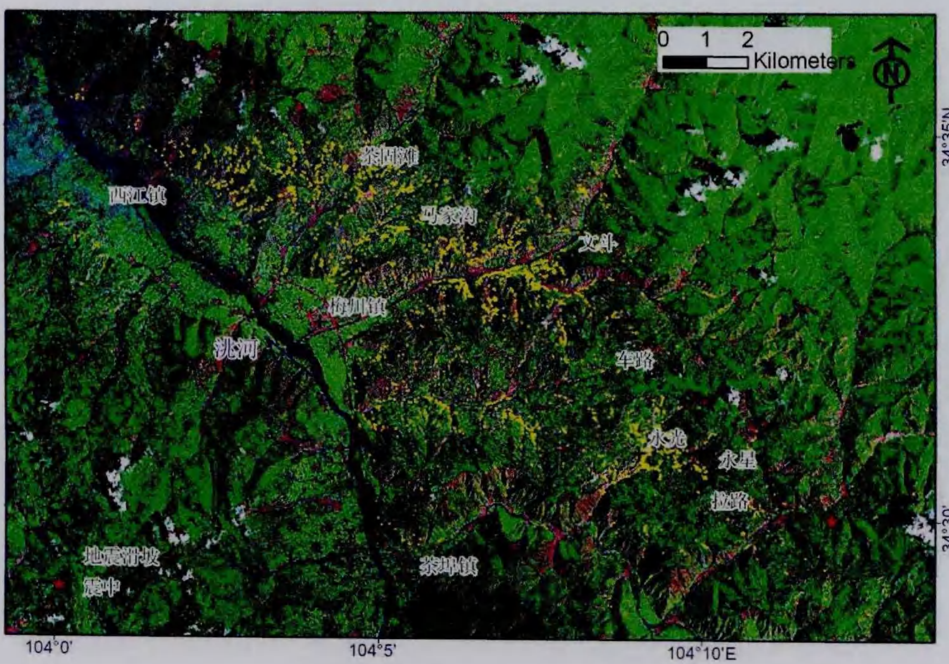

图3 岷县漳县地震触发滑坡分布图

Fig. 3 Distribution of landslides triggered by the Minxian-Zhangxian earthquake

坡度、坡向、斜坡曲率、地层岩性、地震动峰值加速度(PGA)共6个地震滑坡影响因子,依据研究区内各个因子的分布特征和常采用的分类方式,分别对各个因子进行分级。然后分别统计每个因子控制下的滑坡数量,进而得到滑坡在每个因子内的分布情况。

2.1 高程

滑坡在不同高程的发育数量可能存在较大的差异,可能这是由于不同的高程范围的集水区面积、气候、植被覆盖类型不同的原因。研究区内的高程范围为2 207.42~3 340.43 m。为统计不同高程范围的滑坡数量,将研究区内高程按照①2 207.42~2 300 m;②2 300~2 400 m;③2 400~2 500 m;④2 500~2 600 m;⑤2 600~2 700 m;⑥2 700~2 800 m;⑦2 800~2 900 m;⑧2 900~3 000 m;⑨3 000~3 100 m;⑩3 100~3 200 m;⑪3 200~3 340.43 m分为11类,统计这些分类区域内的滑坡分类面积与滑坡数量(图4)。图4的统计结果表明,滑坡的多发高程区间为2 400~2 500 m与2 500~2 600 m。2 600~2 700 m和2 700~2 800 m的高程范围内的高程分类面积最大,但滑坡数量相对较少。高程大于2 800 m的高程范围内滑坡的数量很少。

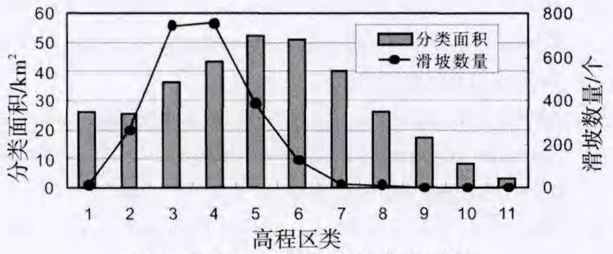

图4　研究区地震滑坡与高程关系

Fig. 4　Correlation of landslide number with elevation

2.2　坡度

斜坡的坡度对滑坡是否发生具有重要的作用。一般情况下，即使没有地震的影响，坡度越大的斜坡也越容易发生滑坡灾害。将研究区坡度按照以下分级进行划分：① 0°~5°、②5°~10°、③10°~15°、④15°~20°、⑤ 20°~25°、⑥ 25°~30°、⑦30°~35°、⑧ 35°~40°、⑨40°~64.6°。统计各个坡度级别内的滑坡分级面积与滑坡数量。统计结果（图5）表明，岷县漳县地震滑坡数量表现出先增加再降低的趋势。呈现这种趋势是因为高坡度的区域范围较小，所以高坡度区域滑坡数量比较小。滑坡数量对应的斜坡坡度峰值为10°~15°范围。

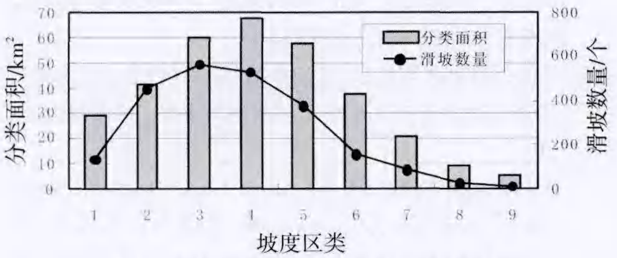

图5　研究区地震滑坡与坡度的关系

Fig. 5　Correlation of landslide number with slope angle

2.3　坡向

以往的研究表明斜坡的坡向对地震滑坡的发生也存在着一定的影响。这可能是由于区域构造应力场方向、地震波传播方向、块体运动方向等对地震滑坡起着一定的作用。按照坡向，将研究区分为①平坦、②北、③北东、④东、⑤ 南东、⑥ 南、⑦ 南西、⑧ 西、⑨北西共9类，不同坡向分级内滑坡数量的统计结果（图6）表明，西与北西方向滑坡数量最多。

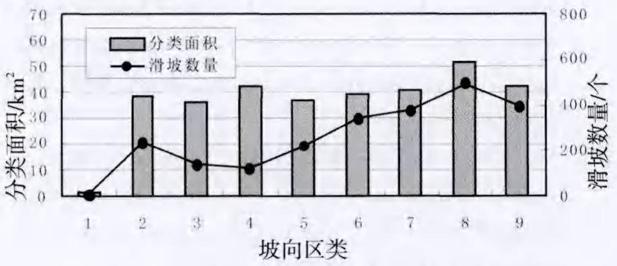

图6　研究区地震滑坡与坡向的关系

Fig. 6　Correlation of landslide number with slope direction

2.4　斜坡曲率

斜坡的曲率也影响地震滑坡的发生。斜坡曲率为正值代表斜坡为凸坡，负值代表斜坡为凹坡，而曲率值为0或接近0的斜坡代表坡面较为平坦。将斜坡曲率分为①<-1、② -1~-0.1、③-0.1~0、④0~0.1、⑤0.1~1、⑥ >1共6类不同的分级，统计每个级别内滑坡数量（图7）。结果表明曲率值范围接近0的斜坡和曲率较大的斜坡，滑坡数量较小。滑坡的多发曲率区间是-1~-0.1。

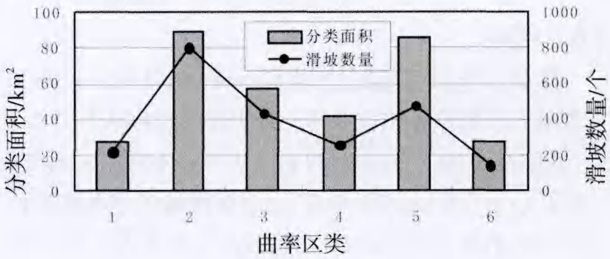

图7　研究区地震滑坡与斜坡曲率的关系

Fig. 7　Correlation of landslide number with slope curvature

2.5　地层岩性

地层岩性对于滑坡变形失稳的影响是显著的，是滑坡发生的物质基础。图8为研究区地层岩性分布图，研究区的地层岩性分为如下几类：①第四系（Q_4、Q_4^{czh}、Q_3）：砾石层、亚砂土、砂质黄土；②新近系（N^b）：粗砂岩、粘土岩、砾岩；③古近系（E^b）：砾岩、砂岩；④二叠系下统（P_1^{1-c}）板岩、砾岩、角砾状灰岩、石英砂岩、粉砂岩；⑤ 二叠系下统（P_1^{1-b}、P_1^{1-a}）：砾岩、含砾石英砂岩、含炭板岩、粉砂岩；⑥ 泥盆系上统（D_3^{dc}）：粉砂质板岩、粉砂岩夹石英砂岩、砾状灰岩；⑦ 泥盆系中统（D_2^{2-e}）：粉砂质板岩、绿泥石板岩、灰质板岩、粉砂岩、灰岩。据研究区地震滑坡数量与岩性的关系图（图9）可知，第③分类古近系（E^b）偶夹砂岩的厚－巨厚层砾岩和块状砾岩滑坡数量最多，属于滑坡多发岩性。

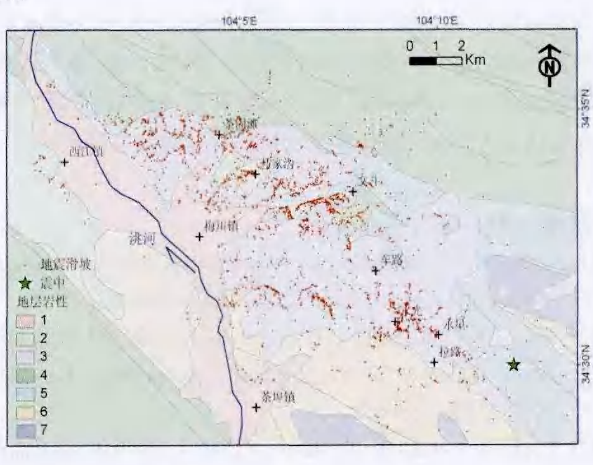

图8　研究区岩性分布图

Fig. 8　Lithology map of the study area

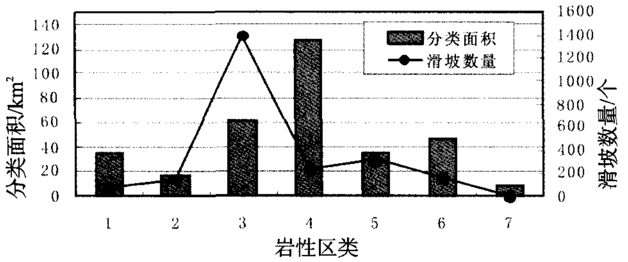

图9 研究区地震滑坡与岩性的关系

Fig. 9 Correlation of landslide number with lithology

2.6 PGA

地震动峰值加速度(Peak Ground Acceleration, PGA)代表地震时地面震动的强度。将研究区内PGA共分为8类,分别为:① 0.34 g,② 0.32 g,③0.28 g,④ 0.24 g,⑤ 0.2 g,⑥ 0.16 g,⑦0.12 g,⑧ 0.08 g。根据滑坡的分类面积和每个分类的滑坡数量,统计出滑坡的空间分布与PGA的关系(图10)。从图10中可以看出滑坡数量最多的PGA值是0.16 g。

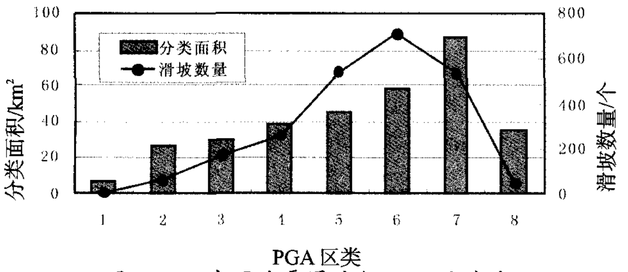

图10 研究区地震滑坡与PGA的关系

Fig.10 Correlation of landslide number with peak ground acceleration

3 结论

岷县漳县地震触发了大量的滑坡。基于高分辨率遥感影像目视解译,并辅以现场调查的方法,得到了2 330处滑坡。对这些地震滑坡的地形、地质与地震特征控制变量进行了分析,包括高程、坡度、坡向、斜坡曲率、地层岩性、PGA共6个特征变量。结果表明:2 400 ~2 600 m的高程范围,10°~20°的坡度,西与北西坡向,-1~-0.1斜坡曲率值范围,古近系(E^b)砾岩与砂岩中,地震动峰值加速度0.16 g是地震滑坡各特征变量的地震滑坡发展区间。

参考文献(References)

[1] Keefer D K. Landslides Caused by Earthquakes[J]. Geological Society of America Bulletin, 1984, 95(4): 406-421.

[2] Pearce A J, O'Loughlin C L. Landsliding during a *M* 7.7 Earthquake: Influence of Geology and Topography[J]. Geology, 1985, 13(12): 855-858.

[3] Pearce A J, Watson A J. Effects of Earthquake-induced Landslides on Sediment Budget and Transport over A 50-yr Period [J]. Geology, 1986, 14(1): 52-55.

[4] Harp E L, Wilson R C, Wieczorek G F. Landslides from the February 4, 1976, Guatemala Earthquake[R]. Washington: US Geological Survey, 1981.

[5] Keefer DK. Statistical Analysis of an Earthquake- induced Landslide Distribution the 1989 Loma Prieta, California Event [J]. Engineering Geology, 2000, 58(3-4): 231-249.

[6] Harp E L, Jibson R W. Landslides Triggered by the 1994 Northridge, California, Earthquake[J]. Bulletin of the Seismological Society of America, 1996, 86(1B): S319-S332.

[7] Wang W N, Wu H L, Nakamura H, et al. Mass Movements Caused by Recent Tectonic Activity: The 1999 Chi-chi Earthquake in Central Taiwan[J]. The Island Arc, 2003, 12(4): 325-334.

[8] Xu C, Xu X W, Yao X, et al. Three (nearly) Complete Inventories of Landslides Triggered by the May 12, 2008 Wenchuan M_W 7.9 Earthquake of China and Their Spatial Distribution Statistical Analysis[J].Landslides,2013,doi:10.1007/s10346-013-0404-6.

[9] 许冲,戴福初,徐锡伟.汶川地震滑坡灾害研究综述[J].地质论评,2010,56(6):860-874.
XU Chong, DAI Fu-chu, XU Xi-wei. Wenchuan Earthquake Induced Landslides: An Overview[J]. Geological Review, 2010, 56(6): 860-874.(in Chinese)

[10] 许冲,徐锡伟,吴熙彦,等.2008年汶川地震滑坡详细编目及其空间分布规律分析[J].工程地质学报,2013,21(1):1-20.
XU Chong, XU Xi-wei, WU Xi-yan, et al. Detailed Inventories of Landslides Triggered by the 2008 Wenchuan Earthquake and Their Spatial Distribution Statistical Analysis[J]. Journal of Engineering Geology, 2013, 21(1): 1-20.(in Chinese)

[11] 侯景瑞,袁中夏.汶川地震滑坡与影响因素[J].西北地震学报,2011,33(S1):398-402.
HOU Jing-rui, YUAN Zhong-xia. Influence Factors of the Landslides Caused by Wenchuan Earthquake[J]. Northwestern Seismological Journal, 2011, 33(S1): 398-402.(in Chinese)

[12] 宋健,高广运,陈青生,等.近断层地震动作用下土质边坡动力响应研究[J].地震工程学报,2013,35(1):62-68.
SONG Jian, GAO Guang-yun, CHEN Qing-sheng, et al. Dynamic Response of Soil Slope under Near-fault Ground Motions[J]. China Earthquake Engineering Journal, 2013, 35(1): 62-68.(in Chinese)

[13] Xu C, Xu X W, Yu G H. Landslides Triggered by Slipping-fault-generated Earthquake on a Plateau: An Example of the 14 April 2010, M_S7.1, Yushu, China Earthquake[J]. Landslides, 2013, 10(4): 421-431.

[14] 许冲,徐锡伟,于贵华.玉树地震滑坡分布调查及其特征

与形成机制[J]. 地震地质, 2012, 34(1): 47-62.
XU Chong, XU Xi-wei, YU Gui-hua. Study on the Characteristics, Mechanism, and Spatial Distribution of Yushu Earthquake Triggered Landslides[J].Seismology and Geology, 2012, 34(1): 47-62.(in Chinese)

[15] 殷跃平, 张永双, 马寅生, 等. 青海玉树M_S7.1级地震地质灾害主要特征[J]. 工程地质学报, 2010, 18(3): 289—296.
YIN Yue-ping, ZHANG Yong-shuang, MA Yin-sheng, et al. Research on Major Characteristics of Geohazards induced by the Yushu M_S7.1 Earthquake[J]. Journal of Engineering Geology, 2010, 18(3): 289-296.(in Chinese)

[16] Gorum T, Van Westen C J, Korup O, et al. Complex Rupture Mechanism and Topography Control Symmetry of Mass-wasting Pattern, 2010 Haiti Earthquake[J]. Geomorphology, 2013, 184: 127-138.

[17] Xu C, Xu X W, Yu G H. Earthquake Triggered Landslide Hazard Mapping and Validation Related with the 2010 Port-au-Prince, Haiti Earthquake[J]. Disaster Advances, 2012, 5 (4): 1297-1304.

[18] 许冲, 徐锡伟. 俯冲带地区压扭断裂型地震触发滑坡及其剥蚀厚度空间分布规律分析[J]. 工程地质学报, 2012, 20 (5): 732-744.
XU Chong, XU Xi-wei. Spatial Distribution of Seismic Landslides and Their Erosion Thickness Relate with a Transpressional Fault Caused Earthquake of Subduction Zone[J]. Journal of Engineering Geology, 2012, 20(5): 732-744.(in Chinese)

[19] 李帅, 许冲, 陈建波, 等. 新疆新源、和静交界M_S6.6地震地质灾害诱发因素浅析[J]. 内陆地震, 2012, 26(4): 365-372.
LI Shuai, XU Chong, CHEN Jian-bo, et al. Analysis on Inducing Factors of Geological Hazard Caused by Xinyuan, Hejing Earthquake with M_S6.6[J]. Inland Earthquake, 2012, 26 (4): 365-372.(in Chinese)

[20] 陈晓利, 袁仁茂, 庾露. Newmark方法在芦山地震诱发滑坡分布预测研究中的应用[J]. 地震地质, 2013, 35(3): 661-670.
CHEN Xiao-li, YUAN Ren-mao, YU Lu. Applying the Newmark's Model in the Assessment of Earthquake-triggered Landslides during the Lushan Earthquake[J]. Seismology and Geology, 2013, 35(3): 661-670.(in Chinese)

[21] 许冲, 肖建章. 2013年芦山地震滑坡空间分布分析——以太平镇东北方向的一个典型矩形区为例[J]. 地震地质, 2013, 35(2): 436-451.
XU Chong, XIAO Jian-zhang. Spatial Analysis of Landslides Triggered by the 2013 M_S 7.0 Lushan Earthquake: A Case Study of a Typical Rectangle Area in the Northeast of Taiping Town[J]. Seismology and Geology, 2013, 35(2): 436-451. (in Chinese)

[22] 许冲, 徐锡伟, 郑文俊, 等. 2013年四川省芦山"4·20"7.0级强烈地震触发滑坡[J]. 地震地质, 2013, 35(3): 641-660.
XU Chong, XU Xi-wei, ZHENG Wen-jun, et al. Landslides Triggered by the April 20, 2013 Lushan, Sichuan Province M_S7.0 Strong Earthquake of China[J]. Seismology and Geology, 2013, 35(3): 641-660.(in Chinese)

[23] 许冲, 徐锡伟, 郑文俊, 等. 2013年甘肃岷县漳县6.6级地震触发滑坡及其构造分析[J]. 地震地质, 2013, 35(3): 616-626.
XU Chong, XU Xi-wei, ZHENG Wen-jun, et al. Landslides Triggered by the 2013 Minxian-Zhangxian, Gansu Province M_S6.6 Eartqhuake and Its Tectonic Analysis[J]. Seismology and Geology, 2013, 35(3): 616-626.(in Chinese)

[24] 郑文俊, 闵伟, 何文贵, 等. 2013年甘肃岷县漳县6.6级地震震害分布特征及发震构造分析[J]. 地震地质, 2013, 35 (3): 604-615.
ZHENG Wen-jun, MIN Wei, HE Wen-gui, et al. Distribution of the Related Disaster and the Causative Tectonic of the Minxian- Zhangxian M_S6.6 Earthquake on July 22, 2013, Gansu, China[J]. Seismology and Geology, 2013, 35(3): 604-615.(in Chinese)

[25] 龚文俊, 李明永, 吴志坚. 降雨和地震耦合作用对滑坡稳定性的影响——以甘肃西和Ⅲ号滑坡为例[J]. 西北地震学报, 2012, 34(2): 161-166.
GONG Wen- jun, LI Ming- yong, WU Zhi- jian. Stability Analysis of Landslide under Coupling Action of Earthquake and Rainfall——Taking the No. III Landslide of Xihe County, Gansu Province as an Example[J]. Northwestern Seismological Journal, 2012, 34(2): 161-166.(in Chinese)

[26] 许冲, 徐锡伟, 郑文俊. 2013年7月22日岷县漳县M_S6.6级地震滑坡编录与空间分布规律分析[J]. 工程地质学报, 2013, 21(5): 736-749.
XU Chong, Xu Xi-wei, ZHENG Wen-jun. Compiling Inventory of Landslides Triggered by Minxian- Zhangxian Earthquake of July 22, 2013 and Their Spatial Distribution Analysis[J]. Journal of Engineering Geology, 2013, 21(5): 736-749. (in Chinese)